AN EFFICIENT MODEL-ORDER REDUCTION APPROACH TO LOW-FREQUENCY TRANSMISSION LINE MODELING

R. Remis

Laboratory of Electromagnetic Research
Faculty of Electrical Engineering, Mathematics and Computer Science
Delft University of Technology
Mekelweg 4, 2628 CD Delft, The Netherlands

Abstract—In this paper, we present a Lanczos-type reduction method to simulate the low-frequency response of multiconductor transmission lines. Reduced-order models are constructed in such a way that low frequencies are approximated first. The inverse of the transmission line system matrix is then required and an explicit expression for this inverse is presented. No matrix factorization needs to be computed numerically. Furthermore, computing the action of the inverse on a vector requires an $O(N)$ amount of work, where N is the total number of unknowns, and the inverse satisfies a particular reciprocity-related symmetry relation as well. These two properties are exploited in a Lanczos-type algorithm to efficiently construct the low-frequency reduced-order models. Numerical examples illustrate the performance of the method.

1. INTRODUCTION

In recent years, Krylov subspace techniques have proven to be valuable tools to simulate the response of multiconductor transmission lines [1–8]. By expanding the currents and voltages around a certain expansion point in frequency, or by expanding the transfer function between a given input and a desired output, accurate current, voltage, or transfer function approximations can obtained on an entire frequency band of interest after only a single run of the underlying Krylov subspace method. The drawback is, however, that for finite expansion points a shifted version of a so-called system matrix needs to be factorized. Computing such a factorization is computationally expensive and we

---

Corresponding author: R. Remis (r.f.remis@tudelft.nl).

like to avoid it whenever possible. In general this can be achieved by taking the expansion point to infinity. For high frequencies or early times such an approach works fine, but if low frequencies or late times are of interest then a large number of iterations may be required to arrive at a satisfactory approximation.

In [9], we showed that for the one-dimensional Maxwell system no factorizations are necessary if frequency zero is taken as an expansion point. Here we extend this low frequency approach to multiconductor transmission lines. To fix ideas, we consider lines characterized by a possibly position dependent per unit length (p.u.l.) capacitance c, inductance ℓ, and resistance r. A voltage generator, consisting of a voltage source $v_s(t)$ in series with a source resistance R_s, is located at the near end of the line and a load consisting of a resistance R_{ld} in series with an inductance $\mathcal{L}_{ld}$ is present at the far end of the line. Although this transmission line model is fairly general, we emphasize that the model-order reduction approach presented here also applies to transmission lines with other line characteristics. Different source and load conditions may be considered, for example. We focus on lines of the above type to present our low-frequency technique and not to clutter the formulas too much by describing every possible transmission line setup that may occur.

For transmission lines in which some loss mechanism is present, we show that the corresponding system matrix is nonsingular and an explicit expression for the inverse of the system matrix is presented as well. This inverse dense (as opposed to the system matrix itself, which is sparse), but computing its action on a given vector still requires an $O(N)$ amount of work, where N is the total number of unknowns. Furthermore, we also show that if the p.u.l. resistance r is uniform along the line and at least one of the resistances r, R_s, or R_{ld} is positive then the system matrix is positive stable (all eigenvalues of the system matrix have a positive real part). Finally, the inverse satisfies a specific symmetry property due to reciprocity and we exploit this property in a Lanczos-type reduction method to efficiently construct the low-frequency approximations for the currents and the voltages along the transmission line. Numerical examples will illustrate the performance of the proposed solution method.

2. STATE-SPACE REPRESENTATION

In this section we consider a transmission line system consisting of a single active conductor only. In Section 4, we generalize to the multiconductor case.

We start with the basic transmission line equations

$$\partial_z v + ri + \ell\partial_t i = 0, \tag{1}$$

and

$$\partial_z i + c\partial_t v = 0, \tag{2}$$

describing the behavior of the voltage v and current i along a single conductor transmission line of length L. To include the presence of the voltage generator at the near end ($z = 0$) of the line we impose the boundary condition

$$v(0, t) = v_s(t) - R_s i(0, t), \tag{3}$$

and since a resistance R_{ld} in series with an inductance $\mathcal{L}_{ld}$ is present at the far end ($z = L$) of the line, we also have

$$v(L, t) = R_{ld} i(L, t) + \mathcal{L}_{ld}\partial_t i(L, t). \tag{4}$$

The voltage source $v_s(t)$ is switched on at $t = 0$ and vanishes prior to this time instant. The voltage and current along the line vanish prior to this time instant as well.

The above equations are discretized in space using standard two-point finite-difference formulas on a nonuniform staggered grid. Specifically, the current i is approximated on a primary grid consisting of n primary nodes. The z-coordinates of these nodes are given by $z_1, z_2, \ldots, z_n$ with $z_1 = 0$, $z_n = L$ and $z_{k+1} > z_k$. The step sizes of the primary grid are defined as $\delta_k = z_{k+1} - z_k$ for $k = 1, 2, \ldots, n - 1$. The voltage v is approximated on a dual grid consisting of $n + 1$ dual nodes. The z-coordinates of these dual nodes are given by $\hat{z}_0, \hat{z}_1, \ldots, \hat{z}_n$ with $\hat{z}_0 = 0$, $\hat{z}_n = L$, and $\hat{z}_k > \hat{z}_{k-1}$. The step sizes of the dual grid are $\hat{\delta}_k = \hat{z}_k - \hat{z}_{k-1}$ for $k = 1, 2, \ldots, n$. The dual nodes interlace with the primary nodes, since we consider a staggered grid. Notice that for a uniform (equidistant) grid with step size δ we have $\hat{\delta}_1 = \delta/2$ and $\hat{\delta}_n = \delta/2$, while all other step sizes are equal to δ in this case.

Approximating the spatial derivatives in Eqs. (1) and (2) by two-point finite-difference formulas and taking into account the boundary conditions of Eqs. (3) and (4), we end up with the state-space representation

$$(\mathbf{D}_r + \mathbf{M}\partial_t)\mathbf{f} = v_s(t)\mathbf{q}, \tag{5}$$

where the field and source vector are given by

$$\mathbf{f} = \left[\mathbf{v}^T, \mathbf{i}^T\right]^T \quad \text{and} \quad \mathbf{q} = \hat{\delta}_1^{-1}\left[\mathbf{0}^T, \left(\mathbf{e}_1^{(n)}\right)^T\right]^T,$$

respectively. The $n - 1$ finite-difference approximations of the voltage are stored in the column vector $\mathbf{v}$ and the n approximations of the

current are stored in the column vector $\mathbf{i}$. Furthermore, $\mathbf{e}_1^{(n)}$ is the first column of the n-by-n identity matrix $\mathbf{I}_n$ (we use the superscript (n) to indicate that $\mathbf{e}_1^{(n)}$ has n elements). The medium matrix is given by

$$\mathbf{M} = \begin{pmatrix} \mathbf{C} & \mathbf{0} \\ \mathbf{0} & \mathbf{L} \end{pmatrix},$$

where the capacitance matrix $\mathbf{C}$ and the inductance matrix $\mathbf{L}$ are given by

$$\mathbf{C} = \operatorname{diag}\left(c\left(\hat{z}_1\right), c\left(\hat{z}_2\right), \ldots, c\left(\hat{z}_{n-1}\right)\right)$$

and

$$\mathbf{L} = \operatorname{diag}\left(\ell\left(z_1\right), \ell\left(z_2\right), \ldots, \hat{\delta}_n^{-1}\mathcal{L}_{ld} + \ell\left(z_n\right)\right),$$

respectively. Furthermore, matrix $\mathbf{D}_r$ is given by

$$\mathbf{D}_r = \begin{pmatrix} \mathbf{0} & \mathbf{Z} \\ \hat{\mathbf{Z}} & \mathbf{R} \end{pmatrix},$$

where $\mathbf{R}$ is the resistance matrix given by

$$\mathbf{R} = \operatorname{diag}\left(\hat{\delta}_1^{-1}R_s + r\left(z_1\right), r\left(z_2\right), \ldots, r\left(z_{n-1}\right), \hat{\delta}_n^{-1}R_{ld} + r\left(z_n\right)\right). \quad (6)$$

Finally, the matrices $\hat{\mathbf{Z}}$ and $\mathbf{Z}$ are bidiagonal differentiation matrices. To give compact explicit expressions for these matrices, we first introduce the $(n-1)$-by-n upper bidiagonal matrix $\operatorname{bidiag}_n(-1, 1)$ with -1 on the diagonal and $+1$ on the upper diagonal. Moreover, we introduce the step size matrices $\mathbf{W}_z$ and $\hat{\mathbf{W}}_z$ as

$$\mathbf{W}_z = \operatorname{diag}\left(\delta_1, \delta_2, \ldots, \delta_{n-1}\right) \quad \text{and} \quad \hat{\mathbf{W}}_z = \operatorname{diag}\left(\hat{\delta}_1, \hat{\delta}_2, \ldots, \hat{\delta}_n\right).$$

The differentiation matrices can now be written as

$$\mathbf{Z} = \mathbf{W}_z^{-1}\operatorname{bidiag}_n(-1, 1) \quad \text{and} \quad \hat{\mathbf{Z}} = -\hat{\mathbf{W}}_z^{-1}\left[\operatorname{bidiag}_n(-1, 1)\right]^T,$$

and it is straightforward to verify that these matrices satisfy the symmetry relation

$$\hat{\mathbf{Z}}^T\hat{\mathbf{W}}_z = -\mathbf{W}_z\mathbf{Z}. \quad (7)$$

Moreover, the null space of matrix $\hat{\mathbf{Z}}$ is trivial, while the null space of matrix $\mathbf{Z}$ is one-dimensional and is spanned by the n-by-1 vector $\mathbf{e}^{(n)} = [1, 1, \ldots, 1]^T$, that is, all vectors in the null space of $\mathbf{Z}$ are of the form $\alpha\mathbf{e}^{(n)}$, where α is a nonzero constant. This result will be used to show that under certain conditions the system matrix is invertible or positive stable or both (see below and the appendix).

3. THE SYSTEM MATRIX AND ITS INVERSE

The state-space representation of Eq. (5) is rewritten in a more convenient form by premultiplying this equation by the inverse of the medium matrix $\mathbf{M}$. We obtain

$$\left(\mathbf{A} + \mathbf{I}_m \partial_t\right) \mathbf{f} = v_s(t) \mathbf{M}^{-1} \mathbf{q}, \tag{8}$$

where we have introduced the system matrix $\mathbf{A}$ as

$$\mathbf{A} = \mathbf{M}^{-1} \mathbf{D}_r \tag{9}$$

and $m = 2n - 1$ is the order of the total system. The system matrix satisfies a particular symmetry property due to reciprocity (see [9] and [10]) which can be used to efficiently construct high-frequency approximations for the voltage and current along the line. Specifically, matrix $\mathbf{A}$ is a so-called $\mathbf{J}$-symmetric matrix, that is, it satisfies the symmetry relation

$$\mathbf{A}^T \mathbf{J} = \mathbf{J}\mathbf{A} \quad \text{with} \quad \mathbf{J}^T = \mathbf{J}. \tag{10}$$

For the single conductor transmission line considered here, we have

$$\mathbf{J} = \begin{pmatrix} \mathbf{CW}_z & \mathbf{0} \\ \mathbf{0} & -\mathbf{L}\hat{\mathbf{W}}_z \end{pmatrix}.$$

Notice that this matrix is diagonal but not positive definite.

In this paper, we are interested in computing low-frequency approximations for the voltage and the current along the transmission line. The inverse of the system matrix is then required and the following theorem shows under what condition this inverse exists.

Theorem: The system matrix is nonsingular if at least one of the diagonal elements of the resistance matrix is positive. The system matrix is singular if the resistance matrix vanishes.

Proof: The system matrix is nonsingular if and only if matrix $\mathbf{D}_r$ is nonsingular. We therefore focus on matrix $\mathbf{D}_r$ and proof that, under the stated condition, $\mathbf{u} = \mathbf{0}$ is the only solution to $\mathbf{D}_r \mathbf{u} = \mathbf{0}$.

We start by writing the resistance matrix as

$$\mathbf{R} = \mathrm{diag}(r_1, r_2, \ldots, r_n),$$

where $r_1 = \hat{\delta}_1^{-1} R_s + r(z_1)$, $r_k = r(z_k)$ for $k = 2, 3, \ldots, n - 1$, and $r_n = \hat{\delta}_n^{-1} R_{ld} + r(z_n)$. Partitioning vector $\mathbf{u}$ conform the partitioning of the field vector $\mathbf{f}$ and writing out $\mathbf{D}_r \mathbf{u} = \mathbf{0}$ in full, we have

$$\begin{pmatrix} \mathbf{0} & \mathbf{Z} \\ \hat{\mathbf{Z}} & \mathbf{R} \end{pmatrix} \begin{pmatrix} \mathbf{u}_v \\ \mathbf{u}_i \end{pmatrix} = \mathbf{0},$$

or

$$\mathbf{Z}\mathbf{u}_i = \mathbf{0} \quad \text{and} \quad \hat{\mathbf{Z}}\mathbf{u}_v + \mathbf{R}\mathbf{u}_i = \mathbf{0}.$$

We have seen that only vectors of the form $\mathbf{u}_i = \alpha\mathbf{e}^{(n)}$ satisfy $\mathbf{Z}\mathbf{u}_i = \mathbf{0}$, where α is a constant. Consequently, we are left with

$$\hat{\mathbf{Z}}\mathbf{u}_v = -\alpha\mathbf{R}\mathbf{e}^{(n)}.$$

Denoting the elements of vector $\mathbf{u}_v$ by $u_{v;k}$ and writing the above equation out in full, we obtain

$$u_{v;k} = -\alpha\sum_{j=1}^{k}\hat{\delta}_j r_j \quad \text{for } k = 1, 2, \ldots, n-1$$

and $u_{v;n-1} = \alpha\hat{\delta}_n r_n$. Taking $k = n-1$ in the above expression, we see that we must have

$$\alpha\hat{\delta}_n r_n = -\alpha\sum_{j=1}^{n-1}\hat{\delta}_j r_j \quad \text{or} \quad \alpha\sum_{j=1}^{n}\hat{\delta}_j r_j = 0.$$

If at least one $r_j > 0$ then $\sum_{j=1}^{n}\hat{\delta}_j r_j > 0$ and the last equation can be satisfied for $\alpha = 0$ only.

The second part of the theorem follows from the fact that matrix $\mathbf{Z}$ has a nontrivial null space.

In all cases of practical interest the condition of the theorem is met and from this moment on we therefore assume that the system matrix is invertible. From Eq. (10) it immediately follows that

$$\mathbf{A}^{-T}\mathbf{J} = \mathbf{J}\mathbf{A}^{-1}, \tag{11}$$

that is, the inverse of the system matrix is also $\mathbf{J}$-symmetric ($\mathbf{J}$-symmetry is closed under inversion). Moreover, in the appendix we show that if the p.u.l. resistance r is uniform along the line and at least one of the resistances r, R_s, or R_{ld} is positive, then the system matrix is positive stable (all its eigenvalues have a positive real part).

Let us now present an explicit expression for the inverse of matrix $\mathbf{A}$. To this end, we first introduce some notation. Introduce the cumulative resistances

$$\nu_k = \sum_{j=1}^{k}\hat{\delta}_j r_j \quad \text{for } k = 1, 2, \ldots, n$$

and let

$$\mathbf{n} = \nu_n^{-1}[\nu_1, \nu_2, \ldots, \nu_{n-1}]^T.$$

Furthermore, let $\mathbf{E}_{kk}$ be the k-by-k matrix of ones and introduce the

integration matrices

$$\mathbf{S}_1 = \begin{pmatrix} \hat{\delta}_1 & 0 & 0 & \cdots & & & & 0 \\ \hat{\delta}_1 & \hat{\delta}_2 & 0 & \cdots & & & & 0 \\ \cdot & \hat{\delta}_2 & \hat{\delta}_3 & 0 & \cdots & & & 0 \\ \cdot & \cdot & \cdot & \cdot & 0 & \cdots & & 0 \\ \cdot & \cdot & \cdot & \cdot & \cdot & 0 & & 0 \\ & & & & & & \hat{\delta}_{n-1} & 0 \\ \hat{\delta}_1 & \hat{\delta}_2 & \cdots & & & & \hat{\delta}_{n-1} & \hat{\delta}_n \end{pmatrix}$$

$$\mathbf{S}_2 = \begin{pmatrix} \hat{\delta}_1 & 0 & 0 & \cdots & & & 0 & 0 \\ \hat{\delta}_1 & \hat{\delta}_2 & 0 & \cdots & & & 0 & 0 \\ \cdot & \hat{\delta}_2 & \hat{\delta}_3 & 0 & \cdots & & 0 & 0 \\ \cdot & \cdot & \cdot & \cdot & 0 & \cdots & 0 & 0 \\ \cdot & \cdot & \cdot & \cdot & \cdot & 0 & 0 & 0 \\ & & & & & \hat{\delta}_{n-2} & 0 & 0 \\ \hat{\delta}_1 & \hat{\delta}_2 & \cdots & & & \hat{\delta}_{n-2} & \hat{\delta}_{n-1} & 0 \end{pmatrix}$$

and

$$\mathbf{S}_3 = \begin{pmatrix} \delta_1 & \delta_2 & \delta_3 & \cdots & \delta_{n-1} \\ 0 & \delta_2 & \delta_3 & \cdots & \delta_{n-1} \\ \cdot & 0 & \delta_3 & \cdots & \delta_{n-1} \\ \cdot & \cdot & & & \\ \cdot & \cdot & & & \\ \cdot & & & & \delta_{n-1} \\ 0 & 0 & \cdots & & 0 \end{pmatrix}.$$

Notice that $\mathbf{S}_1$ is n-by-n, $\mathbf{S}_2$ is $(n-1)$-by-n, and $\mathbf{S}_3$ is n-by-$(n-1)$. With the introduction of all these matrices, we are in a position to present the inverse of matrix $\mathbf{A}$. From its definition, we have

$$\mathbf{A}^{-1} = \mathbf{D}_r^{-1}\mathbf{M},$$

and the inverse of matrix $\mathbf{D}_r$ is given by

$$\mathbf{D}_r^{-1} = \begin{pmatrix} \mathbf{X}_{vv} & \mathbf{X}_{vi} \\ \mathbf{X}_{iv} & \mathbf{X}_{ii} \end{pmatrix}$$

with

$$\mathbf{X}_{ii} = \nu_n^{-1}\mathbf{E}_{nn}\hat{\mathbf{W}}_z, \qquad\qquad \mathbf{X}_{vi} = [\mathbf{I}_{n-1} \mid -\mathbf{n}]\,\mathbf{S}_1,$$
$$\mathbf{X}_{iv} = \mathbf{E}_{n\,n-1}\mathbf{W}_z\mathrm{diag}(\mathbf{n}) - \mathbf{S}_3, \quad \text{and} \quad \mathbf{X}_{vv} = -\mathbf{S}_2\mathbf{R}\mathbf{X}_{iv}.$$

Verifying that this is indeed the correct inverse is straightforward by showing that $\mathbf{A}^{-1}\mathbf{A} = \mathbf{I}_m$. As another check we compute the static voltage and current for a transmission line with a uniform p.u.l.

resistance r. A static voltage and current is obtained by taking a Heaviside step function as a voltage source and by considering the limit $t \to \infty$.

Starting from the general solution of Eq. (8), namely

$$\mathbf{f}(t) = \int_{\tau=0}^{t} \exp[-\mathbf{A}(t - \tau)] v_s(\tau) \, \mathrm{d}\tau \mathbf{M}^{-1}\mathbf{q}, \tag{12}$$

we take $v_s(t) = V_0 H(t)$, where V_0 is a nonzero constant and $H(t)$ is the Heaviside unit step function, and substitute this voltage dependence in Eq. (12) to obtain

$$\mathbf{f}(t) = V_0 \mathbf{A}^{-1} \left[\mathbf{I}_m - \exp(-\mathbf{A}t) \right] \mathbf{M}^{-1}\mathbf{q}.$$

Since matrix $\mathbf{A}$ is positive stable, we have

$$\lim_{t \to \infty} \exp(-\mathbf{A}t) = \mathbf{0},$$

and consequently

$$\begin{pmatrix} \mathbf{v}_{st} \\ \mathbf{i}_{st} \end{pmatrix} := \lim_{t \to \infty} \mathbf{f}(t) = V_0 \mathbf{D}_r^{-1}\mathbf{q}.$$

Substituting the expression for the inverse of matrix $\mathbf{D}_r$ in the above equation and taking $r = 0$ for simplicity, we end up with

$$\mathbf{v}_{st} = V_0 \frac{R_{ld}}{R_s + R_{ld}} \mathbf{e}^{(n-1)} \quad \text{and} \quad \mathbf{i}_{st} = \frac{V_0}{R_s + R_{ld}} \mathbf{e}^{(n)},$$

as it should be, of course. Finally, we observe from the expression for the inverse that computing the matrix-vector product $\mathbf{A}^{-1}\mathbf{u}$ for a given vector $\mathbf{u}$ requires an $O(m)$ amount of work. This allows us to efficiently construct low-frequency reduced-order models via a Lanczos-type reduction algorithm.

4. MULTICONDUCTOR TRANSMISSION LINES

The finite-difference state-space representation for a multiconductor transmission line consisting of $N_T \geq 2$ active conductors is obtained by following a similar approach as for the single conductor line. The spatial coordinate is again discretized on a possibly nonuniform staggered grid and the spatial derivatives are approximated by two-point finite-difference formulas. Just as in the single-conductor case, the resulting state-space representation can be written in the form

$$(\mathbf{D}_r + \mathbf{M}\partial_t)\mathbf{f} = v_{s;k}(t)\mathbf{q}, \tag{13}$$

where this time the field vector is given by

$$\mathbf{f} = \left[\mathbf{v}_1^T, \mathbf{i}_1^T, \mathbf{v}_2^T, \mathbf{i}_2^T, \ldots, \mathbf{v}_{N_T}^T, \mathbf{i}_{N_T}^T \right]^T$$

and $\mathbf{v}_i$ and $\mathbf{i}_i$ are the voltage and current column vectors of the ith conductor. The voltage source of conductor k, $k \in \{1, 2, \ldots, N_T\}$, is active and its signature is denoted by $v_{s;k}(t)$. The source vector is given by

$$\mathbf{q} = \hat{\delta}_1^{-1}\mathbf{e}_j^{(N)},$$

where $N = N_T m$ is the order of the total system, $j = (k-1)m+n$, and $\mathbf{e}_j^{(N)}$ is the jth column of the N-by-N identity matrix $\mathbf{I}_N$. Furthermore,

$$\mathbf{D}_r = \text{diag}(\mathbf{D}_{r;1}, \mathbf{D}_{r;2}, \ldots, \mathbf{D}_{r;N_T}),$$

where

$$\mathbf{D}_{r;j} = \begin{pmatrix} \mathbf{0} & \mathbf{Z} \\ \hat{\mathbf{Z}} & \mathbf{R}_j \end{pmatrix} \quad \text{for } j = 1, 2, \ldots, N_T,$$

and $\mathbf{R}_j$ is the diagonal resistance matrix of the jth conductor. Finally, the medium matrix is given by

$$\mathbf{M} = \begin{pmatrix} \mathbf{M}_{11} & \mathbf{M}_{12} & \cdots & \mathbf{M}_{1N_T} \\ \mathbf{M}_{21} & \mathbf{M}_{22} & \cdots & \mathbf{M}_{2N_T} \\ \vdots & & & \vdots \\ \mathbf{M}_{N_T1} & \mathbf{M}_{N_T2} & \cdots & \mathbf{M}_{N_TN_T} \end{pmatrix},$$

where

$$\mathbf{M}_{ij} = \begin{pmatrix} \mathbf{C}_{ii} & \mathbf{0} \\ \mathbf{0} & \mathbf{L}_{ii} \end{pmatrix} \quad \text{if } j = i \quad \text{and} \quad \mathbf{M}_{ij} = \begin{pmatrix} -\mathbf{C}_{ij} & \mathbf{0} \\ \mathbf{0} & \mathbf{L}_{ij} \end{pmatrix} \quad \text{if } j \neq i.$$

Note that matrix $\mathbf{M}$ is symmetric and positive definite.

We now first multiply Eq. (13) on the left by the inverse of matrix $\mathbf{M}$. Our state-space representation becomes

$$(\mathbf{A} + \mathbf{I}_N \partial_t)\mathbf{f} = v_{s;k}(t)\mathbf{s}, \tag{14}$$

where we again introduced the system matrix as $\mathbf{A} = \mathbf{M}^{-1}\mathbf{D}_r$ and $\mathbf{s} = \mathbf{M}^{-1}\mathbf{q}$.

The system matrix in the multiconductor case is $\mathbf{J}$-symmetric as well. Specifically, let

$$\mathbf{J} = \mathbf{M}\left[\mathbf{I}_{N_T} \otimes \begin{pmatrix} \mathbf{W}_z & \mathbf{0} \\ \mathbf{0} & -\hat{\mathbf{W}}_z \end{pmatrix}\right] = \left[\mathbf{I}_{N_T} \otimes \begin{pmatrix} \mathbf{W}_z & \mathbf{0} \\ \mathbf{0} & -\hat{\mathbf{W}}_z \end{pmatrix}\right]\mathbf{M}, \tag{15}$$

then matrix $\mathbf{A}$ satisfies the symmetry relation $\mathbf{A}^T\mathbf{J} = \mathbf{J}\mathbf{A}$ and clearly $\mathbf{J}^T = \mathbf{J}$. In Eq. (15), $\otimes$ denotes the Kronecker product.

To construct the low-frequency reduced-order models, we need the inverse of the multiconductor system matrix. This inverse is obviously given by

$$\mathbf{A}^{-1} = \mathbf{D}_r^{-1}\mathbf{M},$$

where

$$\mathbf{D}_r^{-1} = \operatorname{diag}\left(\mathbf{D}_{r;1}^{-1}, \mathbf{D}_{r;2}^{-1}, \ldots, \mathbf{D}_{r;N_T}^{-1}\right).$$

Matrix $\mathbf{A}^{-1}$ is $\mathbf{J}$-symmetric, since $\mathbf{J}$-symmetry is closed under inversion. We exploit this symmetry property to efficiently construct the low-frequency reduced-order models for the voltages and the currents.

5. REDUCED-ORDER MODELS

Applying a one-sided Laplace transform to the state-space representation of Eq. (14), we obtain

$$\left(\mathbf{A} + s\mathbf{I}_N\right)\hat{\mathbf{f}} = \hat{v}_{s;k}(s)\mathbf{s}$$

and premultiplying this equation by $\mathbf{A}^{-1}$ gives

$$(\mathbf{I}_N + s\mathbf{A}^{-1})\hat{\mathbf{f}} = \hat{v}_{s;k}(s)\mathbf{A}^{-1}\mathbf{s}. \tag{16}$$

This equation serves as a basis for the construction of the low-frequency reduced-order models. These models are constructed by first generating a $\mathbf{J}$-orthogonal basis of the Krylov subspace

$$\mathbb{K}_p = \operatorname{span}\left\{\mathbf{s}, \mathbf{A}^{-1}\mathbf{s}, \ldots, \mathbf{A}^{-p+1}\mathbf{s}\right\}.$$

The basis vectors are denoted by $\mathbf{v}_1$, $\mathbf{v}_2$, $\ldots$, $\mathbf{v}_p$ and can be computed very efficiently via a three-term Lanczos-type recurrence relation, since $\mathbf{A}^{-1}$ is $\mathbf{J}$-symmetric (see [9–12]). Having the basis vectors available, we approximate the field vector $\hat{\mathbf{f}}(s)$ by the reduced-order model

$$\hat{\mathbf{f}}_p(s) = \hat{\zeta}_1(s)\mathbf{v}_1 + \hat{\zeta}_2(s)\mathbf{v}_2 + \ldots + \hat{\zeta}_p(s)\mathbf{v}_p,$$

which obviously belongs to $\mathbb{K}_p$. Introducing the matrix $\mathbf{V}_p = (\mathbf{v}_1, \mathbf{v}_2, \ldots, \mathbf{v}_p)$ and the vector of expansion coefficients

$$\hat{\mathbf{z}} = \left[\hat{\zeta}_1(s), \hat{\zeta}_2(s), \ldots, \hat{\zeta}_p(s)\right]^T$$

we can also write $\hat{\mathbf{f}}_p(s) = \mathbf{V}_p\hat{\mathbf{z}}$. Substituting this expression in Eq. (16) and applying a Galerkin procedure, the expansion coefficients are found as

$$\hat{\mathbf{z}} = \hat{v}_{s;k}(s)\|\mathbf{s}\|(\mathbf{I}_p + s\mathbf{T}_p)^{-1}\mathbf{T}_p\mathbf{e}_1^{(p)}.$$

In this expression, $\|\mathbf{s}\|$ is the 2-norm of vector $\mathbf{s}$ and $\mathbf{T}_p$ is a p-by-p tridiagonal matrix containing the Lanczos recurrence coefficients. With the above expression for the expansion coefficients, our low-frequency reduced-order model becomes

$$\hat{\mathbf{f}}_p(s) = \hat{v}_{s;k}(s)\|\mathbf{s}\|\mathbf{V}_p(\mathbf{I}_p + s\mathbf{T}_p)^{-1}\mathbf{T}_p\mathbf{e}_1^{(p)}. \tag{17}$$

Notice that for each new frequency s, only a tridiagonal p-by-p matrix needs to be inverted.

We do not have a proof that the model as given by Eq. (17) is passive. However, possible loss of passivity is not an issue here, since we are only interested in the frequency response of the multiconductor transmission line (see, for example, [13]). If the transmission line system is part of a larger passive and possibly nonlinear system and the model is used to replace the transmission line system, then passivity does become an issue. A post-processing technique presented in [13] can detect if passivity is lost and it can modify the reduced-order model such that it becomes passive.

6. NUMERICAL EXPERIMENTS

Our first example is taken from [7]. A transmission line consisting of a single active conductor has the p.u.l. parameters $c = 0.2\,\text{nF/cm}$, $\ell = 0.05\,\text{nH/cm}$, and $r = 0$. The length of the line is $10\,\text{cm}$, $R_s = 1\,\Omega$, and $R_{ld} = 1\,\Omega$ and we are interested in the transfer function $H(s) = v(z = L, s)/v_s(s)$ with $s = j2\pi f$ and $0 \le f \le 9\,\text{GHz}$. Using Eq. (17), the reduced-order model of this transfer function is given by

$$H_p(s) = \|\mathbf{s}\| R_{ld} \left(\mathbf{e}_N^{(N)}\right)^T \mathbf{V}_p \left(\mathbf{I}_p + s\mathbf{T}_p\right)^{-1} \mathbf{T}_p \, \mathbf{e}_1^{(p)}.$$

We use a uniform grid and discretization is chosen such that we have 31 points per smallest wavelength. The order of the total system
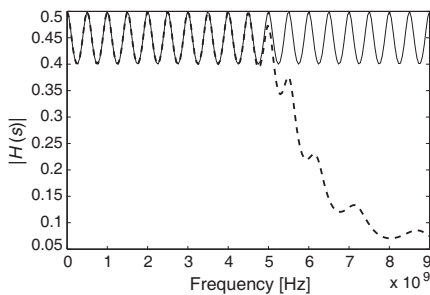

Figure 1. Amplitude of the transmission line transfer function. Solid line signifies the exact result, dashed line is the reduced-order model after $p = 50$ Lanczos iterations.
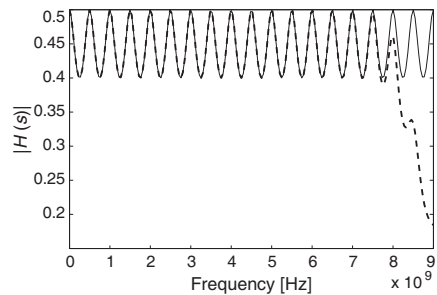
Figure 2. Amplitude of the transmission line transfer function. Solid line signifies the exact result, dashed line is the reduced-order model after $p = 100$ Lanczos iterations.

for this case is $N = 5005$. Figure 1 shows the amplitude of the exact transfer function (solid line) and the amplitude of the reduced-order transfer function after 50 Lanczos iterations (dashed line). We observe that after 50 iterations the response is properly modeled up to approximately 4.5 GHz. Increasing the number of iterations to 100, we obtain the result shown in Figure 2. Clearly, the frequency interval on which the reduced-order model overlaps with the exact result increases with the number of iterations and low frequencies are approximated first. After about 140 iterations the reduced-order model is indistinguishable from the exact result on the frequency band of interest.

In Figure 3, we show the exact response and the reduced-order model obtained after 100 iterations on the same frequency interval as before. This time, however, the source and load resistance are given by $R_s = R_{ld} = 10\,\Omega$. The transfer function has sharp peaks in this case which are captured by the reduced-order model. In addition, if the line is lossy with $r = 10\,\Omega/\text{m}$, we obtain after 100 iterations the result as shown in Figure 4.

In our second example (taken from [6]) we consider a multiconductor transmission line consisting of two active conductors and having a length $L = 0.1\,\text{m}$. The p.u.l. parameters are given by $\ell_{11} = \ell_{22} = 4.03043\,\text{nH/cm}$, $\ell_{12} = \ell_{21} = 0.7696\,\text{nH/cm}$, $c_{11} = c_{22} = 0.4565\,\text{pF/cm}$, $c_{12} = c_{21} = -0.12319\,\text{pF/cm}$, $R_{11} = R_{22} = 0.1\,\Omega/\text{m}$, and $R_{12} = R_{21} = 0$. The 0–10 GHz bandwidth is of interest and
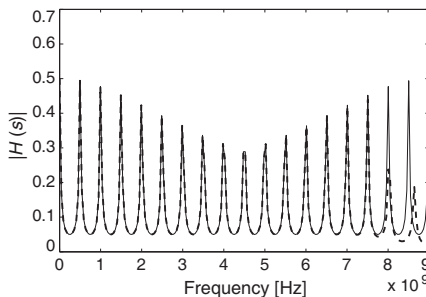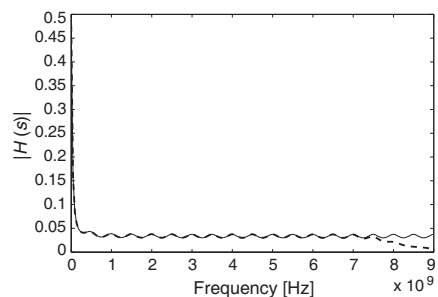

Figure 3. Amplitude of the transmission line transfer function. Solid line signifies the exact result, dashed line is the reduced-order model after $p = 100$ Lanczos iterations. The p.u.l. resistance $r = 0$ and $R_{\mathrm{s}} = R_{ld} = 10\,\Omega$.

Figure 4. Amplitude of the transmission line transfer function. Solid line signifies the exact result, dashed line is the reduced-order model after $p = 100$ Lanczos iterations. The p.u.l. resistance $r = 10\,\Omega/\text{m}$ and $R_{\mathrm{s}} = R_{ld} = 10\,\Omega$.
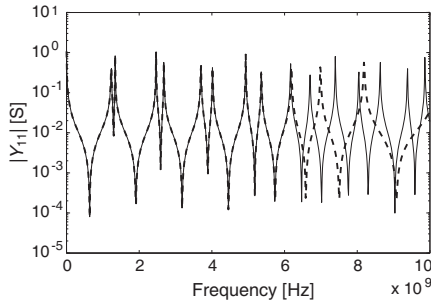
Figure 5. Magnitude of self-admittance of the coupled inter-connect. Solid line reduced-order model after 160 iterations, dashed line reduced-order model after 50 iterations. The reduced-order model of order 160 coincides with the exact solution.
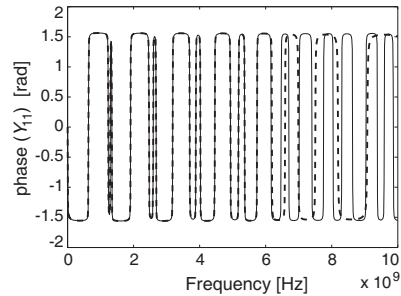
Figure 6. Phase of self-admittance of the coupled inter-connect. Solid line reduced-order model after 160 iterations, dashed line reduced-order model after 50 iterations. The reduced-order model of order 160 coincides with the exact solution.

again discretization is chosen such that we have 31 points per smallest wavelength. If we carry out 50 iterations of the Lanczos-type reduction method and construct the low-frequency reduced-order model we obtain for the magnitude and phase of the self admittance Y_{11} the results shown in Figures 5 and 6 (dashed lines). For the interconnect and frequency bandwidth considered here, the reduced-order models show no noticeable improvement anymore after about 160 Lanczos iterations. The reduced-order model of order 160 for the magnitude and phase of Y_{11} is shown in Figures 5 and 6 as well (solid line). This model coincides with the exact solution for this problem (see also [6]). Again, we observe that low frequencies are approximated first and the interval on which the reduced-order models provide accurate approximations of the self admittance increases with an increasing number of iterations.

7. CONCLUSION

In this paper, we have presented a low-frequency Lanczos-type reduction method for multiconductor transmission lines. Reduced-order models were constructed by iterating with the inverse of the transmission line system matrix in a Lanczos-type algorithm. This algorithm exploits a particular symmetry property of the system matrix and only a single matrix-vector product needs to be computed

at every iteration. Computing such a product requires an $O(N)$ amount of work, where N is the total number of unknowns. The overall method is therefore very efficient if low frequencies are of interest.

As we mentioned in the Introduction, the low-frequency approach presented here can be applied to other types of transmission lines as well. For example, if a conductance matrix $\mathbf{G}$ and a resistance matrix $\mathbf{R}$ are present, the system matrix becomes

$$\mathbf{A} = \mathbf{M}^{-1} \begin{pmatrix} \mathbf{G} & \mathbf{Z} \\ \hat{\mathbf{Z}} & \mathbf{R} \end{pmatrix}$$

and the inverse of this matrix is given by

$$\mathbf{A}^{-1} = \begin{pmatrix} \mathbf{G}^{-1} + \mathbf{G}^{-1}\mathbf{Z}\mathbf{K}^{-1}\hat{\mathbf{Z}}\mathbf{G}^{-1} & -\mathbf{G}^{-1}\mathbf{Z}\mathbf{K}^{-1} \\ -\mathbf{K}^{-1}\hat{\mathbf{Z}}\mathbf{G}^{-1} & \mathbf{K}^{-1} \end{pmatrix} \mathbf{M},$$

where $\mathbf{K} = \mathbf{R} - \hat{\mathbf{Z}}\mathbf{G}^{-1}\mathbf{Z}$. Observe that $\mathbf{K}$ is nonsingular and satisfies $\mathbf{K}^T\hat{\mathbf{W}}_z = \hat{\mathbf{W}}_z\mathbf{K}$, that is, matrix $\mathbf{K}$ is symmetric with respect to $\hat{\mathbf{W}}_z$. Obviously, if the conductance matrix $\mathbf{G}$ vanishes then the above expression for $\mathbf{A}^{-1}$ cannot be used. In this case the inverse of matrix $\mathbf{A}$ does exist, of course, and an explicit expression for the inverse is given in the main text.

Constructing low-frequency reduced-order models requires iterating with the inverse of the system matrix, while high-frequency approximations can be obtained by iterating with the system matrix itself. Since computing matrix-vector products is fast, it makes sense to setup a Lanczos-type reduction method by which we can generate reduced-order models that approximate the low- and high-frequency content of the solution simultaneously. Future work focusses on developing such a method for frequency- and time-domain problems.

ACKNOWLEDGMENT

APPENDIX A. POSITIVE STABILITY OF THE SYSTEM MATRIX

We show that if at least one of the resistances R_s, R_{ld}, or r is positive then the system matrix $\mathbf{A}$ is positive stable (all its eigenvalues

have a real part greater than zero). To this end, we first consider the eigenproblem for the system matrix when all resistances vanish. Denoting the system matrix in this case by $\tilde{\mathbf{A}}$, we have

$$\tilde{\mathbf{A}} = \mathbf{M}^{-1} \begin{pmatrix} \mathbf{0} & \mathbf{Z} \\ \hat{\mathbf{Z}} & \mathbf{0} \end{pmatrix} \tag{A1}$$

and we write its eigenproblem as

$$\begin{pmatrix} \mathbf{0} & \mathbf{Z} \\ \hat{\mathbf{Z}} & \mathbf{0} \end{pmatrix} \begin{pmatrix} \mathbf{x}_v \\ \mathbf{x}_i \end{pmatrix} = \lambda \mathbf{M} \begin{pmatrix} \mathbf{x}_v \\ \mathbf{x}_i \end{pmatrix}. \tag{A2}$$

For $\lambda = 0$ we satisfy the above equation for $\mathbf{x}_v = \mathbf{0}$ and $\mathbf{x}_i = \alpha \mathbf{e}^{(n)}$, where α is a nonzero constant. This shows that the current part of the eigenvector does not vanish. In particular, we have $\mathbf{x}_{i;1} \neq 0$ and $\mathbf{x}_{i;n} \neq 0$, that is, the first and last components of $\mathbf{x}_i$ do not vanish. This latter property carries over to eigenvectors corresponding to nonzero eigenvalues. More precisely, if $(\lambda, \mathbf{x})$ is an eigenpair of $\tilde{\mathbf{A}}$ and $\lambda \neq 0$ then we also have $\mathbf{x}_{i;1} \neq 0$ and $\mathbf{x}_{i;n} \neq 0$. To see this, assume the opposite and let $\mathbf{x}_{i;1} = 0$, or $\mathbf{x}_{i;n} = 0$, or both. It then follows from the eigensystem of Eq. (A2) that $\mathbf{x}$ must be the zero vector, but the zero vector cannot be an eigenvector. In conclusion, for all eigenvectors of matrix $\tilde{\mathbf{A}}$ we have $\mathbf{x}_{i;1} \neq 0$ and $\mathbf{x}_{i;n} \neq 0$.

To proof the positive stability property of matrix $\mathbf{A}$, we make use of the following theorem presented in [14].

Theorem: Let $\mathbf{A}$ be a square and real matrix and suppose that $\mathbf{GA} + \mathbf{A}^T \mathbf{G} = \mathbf{H}$ for some positive definite $\mathbf{G}$ and some positive semidefinite $\mathbf{H}$ and let $\mathbf{S} = \mathbf{GA} - \mathbf{A}^T \mathbf{G}$. Then $\mathbf{A}$ is positive stable if and only if no eigenvector of $\mathbf{G}^{-1} \mathbf{S}$ lies in the null space of $\mathbf{H}$.

We apply this theorem to our problem. Let $\mathbf{A}$ be the system matrix and take $\mathbf{G} = \mathbf{WM}$. Matrix $\mathbf{G}$ is clearly positive definite and

$$\mathbf{H} = 2 \begin{pmatrix} \mathbf{0} & \mathbf{0} \\ \mathbf{0} & \mathbf{R}\hat{\mathbf{W}}_z \end{pmatrix},$$

showing that $\mathbf{H}$ is positive semidefinite. Moreover, $\mathbf{G}^{-1} \mathbf{S} = 2\tilde{\mathbf{A}}$, where $\tilde{\mathbf{A}}$ is the lossless system matrix given by Eq. (A1). Now let $\mathbf{x}$ denote an eigenvector of this matrix and let at least one of the resistances R_s, R_{ld}, or r be positive. Then the first or last element on the diagonal of matrix $\mathbf{R}$ does not vanish (or both do not vanish, see Eq. (6)) and

$$\mathbf{Hx} = 2 \begin{pmatrix} \mathbf{0} \\ \mathbf{R}\hat{\mathbf{W}}_z \mathbf{x}_i \end{pmatrix} \neq \mathbf{0},$$

since we know that $\mathbf{x}_{i;1} \neq 0$ and $\mathbf{x}_{i;n} \neq 0$. This shows that no eigenvector of $\mathbf{G}^{-1} \mathbf{S}$ is in the null space of $\mathbf{H}$ and we conclude that the system matrix is positive stable.

REFERENCES

1. Odabasioglu, A., M. Celik, and L. T. Pileggi, "PRIMA: Passive reduced-order interconnect macromodeling algorithm," *IEEE Trans. on Computer-aided Design of Integrated Circuits and Systems*, Vol. 17, No. 8, 645–654, Aug. 1998.

2. Pasha, S., A. C. Cangellaris, and J. L. Prince, "An all-purpose dispersive multiconductor interconnect model compatible with PRIMA," *IEEE Trans. on Advanced Packaging*, Vol. 24, No. 2, 126–131, May 2001.

3. Cangellaris, A. C., M. Celik, S. Pasha, and L. Zhao, "Electromagnetic model order reduction for system-level modeling," *IEEE Trans. Microwave Theory Tech.*, Vol. 47, No. 6, 840–850, Jun. 1999.

4. Ruehli, A. E. and A. C. Cangellaris, "Progress in the methodologies for the electrical modeling of interconnects and electronic packages," *Proceedings of the IEEE*, Vol. 89, No. 5, 740–771, May 2001.

5. Gunupudi, P. K., M. Nakhla, and R. Achar, "Simulation of high-speed distributed interconnects using Krylov-space techniques," *IEEE Trans. on Computer-aided Design of Integrated Circuits and Systems*, Vol. 19, No. 7, 799–808, Jul. 2000.

6. Cangellaris, A. C. and M. Igarashi, "Rules for robust generation of accurate reduced-order models for high-speed coupled interconnections," *IEEE Transactions on Advanced Packaging*, Vol. 24, No. 2, 120–125, May 2001.

7. Celik, M. and A. C. Cangellaris, "Simulation of multiconductor transmission lines using krylov subspace order-reduction techniques," *IEEE Transactions on Computer-aided Design of Integrated Circuits and Systems*, Vol. 16, No. 5, 485–496, May 1997.

8. Khalaj-Amirhosseini, M., "Closed form solutions for nonuniform transmission lines," *Progress In Electromagnetics Research B*, Vol. 2, 243–258, 2008.

9. Remis, R. F., "Low-frequency model-order reduction of electromagnetic fields without matrix factorization," *IEEE Trans. Microwave Theory Tech.*, Vol. 52, No. 9, 2298–2304, Sep. 2004.

10. Remis, R. F. and P. M. Van Den Berg, "A modified Lanczos algorithm for the computation of transient electromagnetic wavefields," *IEEE Trans. Microwave Theory Tech.*, Vol. 45, 2139–2149, Dec. 1997.

11. Freund, R. W., "Lanczos-type algorithms for structured non-Hermitean eigenvalue problems," *Proc. Cornelius Lanczos Int.*

Centenary Conf., 243–245, 1993.

12. Freund, R. W. and N. M. Nachtigal, "Software for simplified Lanczos and QMR algorithms," *Appl. Numer. Math.*, Vol. 19, 319–341, 1995.

13. Bai, Z., "Krylov subspace techniques for reduced-order modeling of large-scale dynamical systems," *Appl. Numer. Math.*, Vol. 43, 9–44, 2002.

14. Horn, R. A. and C. R. Johnson, *Topics in Matrix Analysis*, Cambridge University Press, Cambridge, 1994.